New insights into long-term chloride transport in unsaturated cementitious materials Role of degree of water saturation

Zhang, Yong; Ye, Guang; Yang, Zhengxian

DOI
10.1016/j.conbuildmat.2019.117677

Publication date
2020

Document Version
Accepted author manuscript

Published in
Construction and Building Materials

Citation (APA)
Zhang, Y., Ye, G., & Yang, Z. (2020). New insights into long-term chloride transport in unsaturated cementitious materials: Role of degree of water saturation. *Construction and Building Materials*, *238*, Article 117677. https://doi.org/10.1016/j.conbuildmat.2019.117677

New insights into long-term chloride transport in unsaturated cementitious materials: Role of degree of water saturation

Yong Zhang [a,b,c], Guang Ye [c], Zhengxian Yang [a,b,*]

[a] Fujian Provincial University Research Center for Advanced Civil Engineering Materials, Fuzhou University, Fuzhou 350116, China;

[b] College of Civil Engineering, Fuzhou University, Fuzhou 350116, China;

[c] Microlab, Section of Materials and Environment, Faculty of Civil Engineering and Geosciences, Delft University of Technology, 2628 CN Delft, the Netherlands; y.zhang-1@tudelft.nl (Yong Zhang), g.ye@tudelft.nl (Guang Ye)

* Correspondence: Zhengxian Yang (zxyang@fzu.edu.cn), College of Civil Engineering, Fuzhou University

Abstract: Concrete is rarely saturated. Reliable durability design of marine concrete structures requires a solid understanding of the long-term chloride transport in unsaturated concretes. This paper presents a critical analysis of the time-dependent chloride diffusion coefficient in unsaturated cementitious materials exposed to marine environment. Evolutions of pore structure and chloride diffusion coefficient in saturated cementitious materials, along with the role of the degree of water saturation in long-term chloride diffusion, are analyzed. It is emphasized that the long-term sharp decrease of the chloride diffusion coefficient in marine cementitious materials is not primarily caused by densification of the microstructure due to hydration, but by the decreasing degree of water saturation with depth in the surface part of the materials. The effects of water/binder ratio and supplementary cementitious materials on chloride diffusion coefficient are different between saturated and unsaturated cementitious materials.

Keywords: Cementitious material; Chloride; Degree of water saturation; Pore structure; Long-term transport

1. Introduction

The present paper constitutes one part of a series of several interrelated papers devoted to examining the chloride transport in unsaturated concretes [1-4]. It is hoped that these papers, taken together, can constitute a coherent conceptual framework that enables to understand the chloride transport in a manner approaching to the realistic situation, and that it will provide a scientific background for service life prediction based on unsaturated chloride transport.

1.1 Chloride diffusion in concrete

Today, more than ever, the governments and the owners want to be assured of the long-term performances of the reinforced concrete infrastructures with life expectancy over 100 years. Chloride penetration is an issue of primary concern in service life design. In present service life calculations, the chloride penetration in concrete structures, exposed to stable marine conditions such as submerged, tidal, splash zone, etc., is normally considered to be controlled by diffusion. Diffusion of chloride ions takes place, under a concentration gradient, via the continuous water-filled pores in concrete [2]. A certain percentage of the chloride ions interacts with the binder in terms of physical adsorption to e.g. calcium silicate hydrates [5], and chemical bound to aluminates as Friedel's salt or Kuzel's salt, and even reacts with calcium hydroxide [6]. The so-called free or water-soluble chlorides, which diffuse inwards, are detrimental to the reinforcement corrosion. The chloride diffusion coefficient, derived by using Fick's second law to describe the chloride profiles, was often used for service life design of reinforced concrete structures located in chloride-laden environments.

Considerable efforts have been dedicated to clarifying the fundamental aspects of chloride diffusion in saturated and non-saturated concretes [5-28]. The difficulties linked to accurate description of chloride diffusion can be attributed to the intrinsic complexity of the concrete microstructure and to the sophistication of the moisture condition (moisture content and its distribution), as well as to the intricate nature of the diffusion phenomena. In principle Fick's law of diffusion is valid only for non-ionic substances. For ionic diffusion the ion-ion interactions need to be involved accounting for the increase of diffusion with dilution. Tang [7,8] has proved a strongly concentration dependent chloride diffusion coefficient after a series of theoretical and experimental investigations. The chloride ions at the penetration front are mostly free. With ongoing penetration process accumulations of the chloride ions take place, resulting in a larger chloride binding, until saturation of chloride content is attained [9]. Diffusion of chloride ions is always accompanied with the movement of cations

in order to keep the electric charges balanced in the pore solution. The diffusivity of chloride (Cl^-) is larger than that of sodium (Na^+) [27]. When a concrete is exposed to an aqueous solution of NaCl, the cations (e.g. calcium Ca^{2+}) can move to the down-stream side along with the Cl^- and the hydroxyl (OH^-) will move to the up-stream side without any imposed concentration gradients [28]. The electrical double layer (EDL) formed on the particle surface plays an important part in chloride diffusion [29]. Hydrated cement particles are negatively charged so that the cations are more concentrated in the EDL than in the bulk solution. Cl^- and Ca^{2+} are forced to diffuse together so that the diffusivity of Cl^- in the bulk solution is retarded and that of Ca^{2+} in the EDL is accelerated. The EDL effect on chloride diffusion is more pronounced in the smaller water-filled pores [3].

1.2 Long-term chloride diffusion

Laboratory measurements and field data have demonstrated that the chloride diffusion coefficient is not a constant but decreases with time. Takewake and Mastumoto [30] maybe the first who pointed out the time-dependency of chloride diffusion in concrete. A wide range of experimental data on this subject was reported by Mangat and Molloy [31]. Tang and Nilsson [32] proposed an expression, according to Crank's mathematics of diffusion, to quantify the decrease of chloride diffusion coefficient with age. Current service life design, e.g. DuraCrete [33], relies on the time-dependent chloride diffusion coefficient $D(t)$, which is described with a power equation:

$$D(t) = D_0 \cdot \left(\frac{t_0}{t}\right)^n \tag{1}$$

where n is the ageing factor, which stands for the decrease of chloride diffusion coefficient with age. The $D(t)$ is extremely sensitive to small changes in the ageing factor n. D_0 is a constant referring to the chloride diffusion coefficient at a reference age t_0 (often t_0 = 28 days). The unsaturated state has been a significant obstacle for standardization of the measurement of the chloride diffusion coefficient in unsaturated concretes [2]. In practice the D_0-value is usually determined based on chloride penetration testes (e.g. NT Build 492 [34]) of concrete specimens after vacuum saturation.

Densification of the microstructure due to continuous cement hydration has been long time considered an explanation for the decrease of the chloride diffusion coefficient $D(t)$ [14], and it is generally regarded as the main source used for determining the ageing factor n. It has been recognized, however, that the cement hydration is noticeable only in the first few

years [35]. A long-term sharp decrease in the $D(t)$ value caused merely by cement hydration is virtually inconceivable.

In the absence of long-term exposure data, determination of the ageing factor n largely depends on our knowledge about evolutions of the chloride diffusion coefficient D measured from laboratory specimens. Plenty of reports on this topic are available [36-38]. These reports are generally based on regression analyses on experimental data, i.e. by using Eq. (1) to fit the time-related chloride diffusion coefficient D measured from rapid chloride migration (RCM) tests of concrete specimens. An example is provided in Fig. 1. An ageing factor n = 0.0513 is obtained for the OPC concrete prepared under laboratory condition. In the DuraCrete [33], however, the ageing factor n is considerably larger, i.e. n = 0.30 for submerged OPC concrete and n = 0.65 for atmospheric OPC concrete. Obviously, the diffusion coefficient D obtained from RCM tests of laboratory concretes shows a relatively slow decrease with age, whereas the D-value predicted from the DuraCrete drops to a great extent with age. Such significant differences in long-term chloride diffusion prediction have been noticed for a long time [36]. One uttermost reason can be ascribed to the fact that a well-prepared laboratory concrete specimen for RCM test is almost *saturated* while onsite concrete is usually *unsaturated* owing to self-desiccation and/or wetting-drying cycles [1]. This makes it essential to consider a point, not explicitly addressed so far, namely that the chloride diffusion coefficient $D(t)$ can decrease with decreasing moisture content.

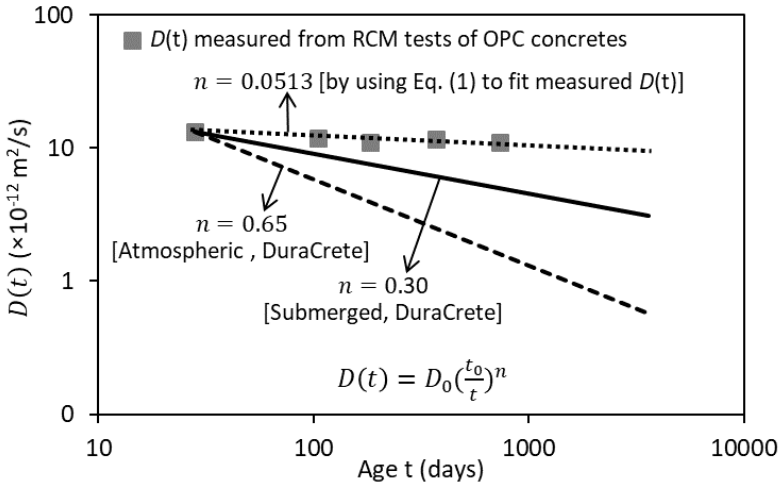

Fig. 1 Evolution of the chloride diffusion coefficient $D(t)$ in OPC concretes (water/cement = 0.5) predicted based on different ageing factor n.

Fig. 2 shows an example of the moisture profile in the marine concrete. The near-surface part may have a high degree of water saturation S_w because of the moisture ingression from ambient environment. The internal concrete (Zone II), however, is relatively dry and has a saturation level S_w approximately the same as that caused by self-desiccation [39,40]. There is a moisture gradient in Zone I. The capillary absorption, owing to wetting-drying cycles, can accelerate the chloride penetration in cover concrete for the first few years of exposure. The absorption effect is strong when the moisture content of the near-surface concrete is low, but becomes increasingly weak with an increase of the wetting-drying cycles, since wetting-drying cycles normally lead to a continuous water supply and comparatively little evaporation [41,42]. In cases where high performance concretes are used, the influential depth of wetting-drying cycles will be limited only to the outermost part of the concrete and will play insignificant role in chloride penetration in the internal concrete [43]. During wetting and drying, there is a balance between water loss and intake after an equilibrium wetting-drying time ratio is reached [42]. The chloride penetration in Zone II is considered driven merely by diffusion.

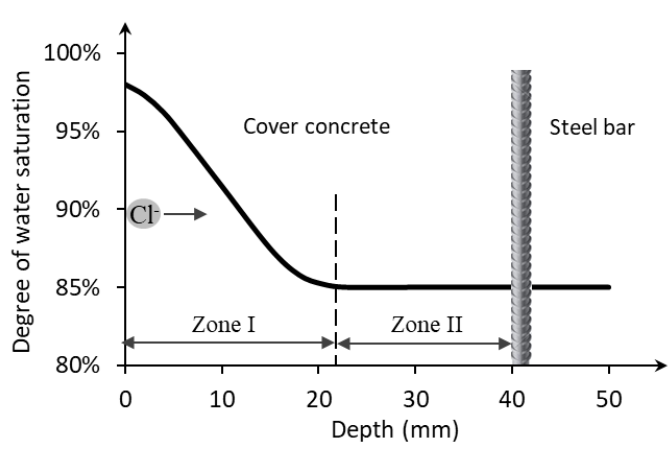

Fig. 2 An example of the moisture profile in concrete after 2-year exposure to marine environment and transport of chloride (Cl^-) [40,44].

1.3 Research significance

A critical review on models and equations regarding the time-dependence of chloride diffusion has been reported by Nilsson [18]. These models/equations may be useful in many practical applications, but they will fail, wholly or in part, when used for predictions of large-scale concrete infrastructures with a long-expected service life. The main weaknesses of these models/equations are the ignorance of the influences of moisture content on long-term

chloride penetration. Interestingly most of the concrete structures built in recent decade are of low water/binder ratio and the internal moisture content is low. Supplementary cementitious materials, widely incorporated into concrete to meet sustainable development goals, may also reduce the moisture content in concrete [45]. The microclimate, i.e. profile of the degree of water saturation S_w, should be a key element involved in the ageing factor n. Disregarding the microclimate implies that the models/equations are, by definition, inadequate to describe the chloride diffusion, and can give rise to misinterpretations of observed transport phenomena.

Chatterji [46], from a series of experimental studies, reported an obvious drop of chloride diffusion coefficient after a comparatively short interval of rapid chloride penetration and explained as due to the unsaturated state of concrete, i.e. water content decreases with depth. Nilsson [47] observed a similar trend of a very slow chloride penetration after an initial rapid rate based on examinations of under-water concrete structures. Chrisp et al. [48] found a decrease of electrical conductivity with depth owing to a gradient of the moisture content in cover concrete. The need for caution and concern with respect to inaccurate prediction of long-term chloride diffusion is apparent. Correct understanding of the unsaturated state, and hence an appropriate description of the time-dependent unsaturated chloride diffusion, are essential for reliable service life prediction of marine concrete structures.

The time-dependency of chloride diffusion in marine concrete is influenced by many factors. The present work deals with the analysis of the role of the degree of water saturation, a key influencing factor, in long-term chloride diffusion. An analytical model previously reported in Ref. [3] will be extended to analyze the time-dependent chloride diffusion coefficient $D(t)$ in unsaturated cementitious materials. Effects of the degree of water saturation on $D(t)$ are discussed in depth. The results will be compared with those determined from the well-known DuraCrete model, in order to ensure the reliability and the efficiency of the proposed approach. A deep insight into the effect of unsaturated state on the time-dependent chloride diffusion will help to predict the service life towards a scientific manner, rather than merely based on long-term exposure data.

2. Time-dependent unsaturated chloride diffusion

Chloride diffusion in a cementitious system is mainly determined by the moisture content (degree of water saturation S_w) and the microstructure (changing with the degree of hydration α). With the addition of supplementary cementitious materials, the hydration process becomes complicated. Accurate determination of the α of each raw material is far from easy.

Nevertheless, the α value in the entire cementitious system, by fitting against relative non-evaporable water content, can generally be formulated with the expression proposed by Jonasson [49]:

$$\alpha(t) = \exp[-a(\ln t)^{-b}] \quad (2)$$

where t is the age; a and b are fitting positive parameters.

An example of the hydration curve according to Eq. (2) is shown in Fig. 3. The curve indicates that the degree of hydration $\alpha(t)$ shows limited change after a reference age t_{ref}. The change of the microstructure at later ages ($t > t_{\mathrm{ref}}$) is small. In the following the evolution of the chloride diffusion will, therefore, not be described as a function of the degree of hydration $\alpha(t)$, but described instead as a function of the degree of water saturation S_{w}.

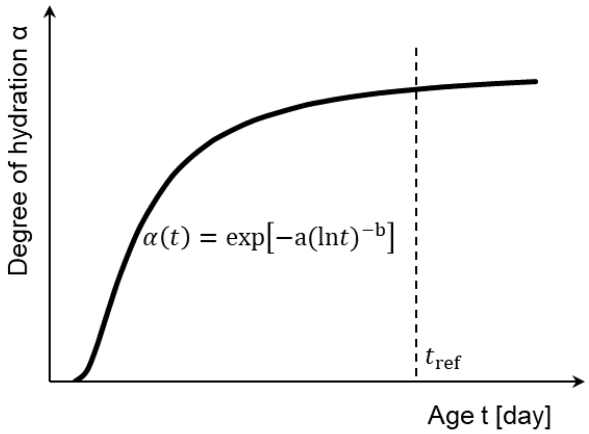

Fig. 3 Changes of the degree of hydration with age in cementitious systems.

In previous work [3] a model of the chloride diffusion coefficient at various degrees of water saturation S_{w} has been proposed. Here this model is extended considering the material age t. The time-dependent unsaturated chloride diffusion coefficient can then be formulated as:

$$D(t, S_{\mathrm{w}}) = D_{\mathrm{Sat}}(t) \cdot S_{\mathrm{w}} \cdot \exp\left[\frac{(1-S_{\mathrm{w}})^2}{2\cdot[0.01 d_{\mathrm{a}}(t)-0.05]^2}\right] \quad (3)$$

where:

- S_{w} [-] is the degree of water saturation. The S_{w} value can change with self-desiccation and/or moisture exchange with ambient environment.

- $D(t, S_w)$ [m^2/s] is the chloride diffusion coefficient in the unsaturated cementitious material. The $D(t, S_w)$ value changes with time t and degree of water saturation S_w.
- $D_{Sat}(t)$ [m^2/s] is the chloride diffusion coefficient of the cementitious material at saturated state, which can be obtained from resistivity measurements, steady-state diffusion or migration cell methods. The D_{Sat} value usually decreases with increasing degree of hydration α in the cementitious material.
- $d_a(t)$ [nm] is the average pore diameter, which can be obtained from mercury porosimetry measurements. The d_a value usually decreases with increasing degree of hydration α in the cementitious material.

To understand the $D(t, S_w)$, experiments will be carried out to examine the values of $D_{Sat}(t)$ and $d_a(t)$. Regarding the time-dependency of the degree of water saturation $S_w(t)$, a simple discussion will be provided afterwards in the comparative study.

3. Experimental

3.1 Materials and samples

Cement paste and mortar samples according to European Standard EN 196-1 were cast. Details of the mixture proportions for the binders are listed in Table 1. CEM I 42.5 N (OPC) was the essential part in all the binders under study. Supplementary cementitious materials (SCMs) with typical replacement levels were studied, i.e. 30% for fly ash (FA), 70% for ground granulated blast furnace slag (BFS) and 5% for limestone powder (LP). Three different water/binder (w/b) ratios were considered, i.e. 0.4, 0.5 and 0.6. Paste and mortar samples were cured in a humid room at 20 ± 0.1 ˚C.

Table 1 Mixture proportions used for the binders.

Mixtures	Raw materials and replacement by weight				w/b
	OPC	FA	BFS	LP	
M4	100%	-	-	-	0.4
M5	100%	-	-	-	0.5
M6	100%	-	-	-	0.6
MF5	70%	30%	-	-	0.5
MB5	30%	-	70%	-	0.5
MFL5	65%	30%	-	5%	0.5

The paste samples at desired ages were crushed into small pieces (around 1 cm^3). The small pieces were moved into liquid nitrogen to stop hydration and then placed in a freeze-drier with -24 ˚C and under vacuum at 0.1 Pa. After the mass loss was below 0.01% per day, the paste pieces were used for pore structure measurements. The mortar samples were made with the same amount of siliceous sand but varied with paste mixtures. Standard quartz sand 0-2 mm (EN 196-1) with a density of 2.63 g/cm^3 was used as aggregate. The paste/sand ratio was fixed at 1:3 by weight. All mortar samples were moist-cured for desired ages before they were used for rapid chloride migration tests.

3.2 Pore structure characterization

Mercury intrusion porosimetry (MIP) was applied for characterizing the pore structure of various cementitious pastes. The paste specimens were at the ages of 28, 105, 182 and 370 days. MIP measurements were performed with Micromeritics PoreSizer® 9320. Each measurement was conducted in two stages: a manual low pressure run from 0 to 0.15 MPa and an automated high pressure run from 0.15 to 210 MPa. The raw data produced from mercury intrusion were calculated by using the Washburn equation [50], with a contact angle of 139º and a surface tension of mercury of 0.48 N/m^2. The minimum pore diameter hence measured by the apparatus was 7 nm. The dried paste specimens used for MIP were in the range of 4～8 g by mass with the expectation that the intrusion volume of mercury was about 60～90% of the stem volume in complying with the regulations of the apparatus. Due to the ink-bottle effect, MIP measurements tend to underestimate the large pores and overestimate the small pores [51]. In this study, MIP was utilized with the main purpose to monitor the trend of the pore size changes with age due to hydration.

For the total pore volume V_t [m^3/m^3] and total surface area S_t [m^2/m^3] of the pores, the average pore diameter d_a is calculated as [3]:

$$d_a = \frac{4V_t}{S_t} \tag{4}$$

3.3 Rapid chloride migration tests

Rapid chloride migration (RCM) tests were carried out on mortar specimens (ϕ100×50 mm) according to the method described in NT Build 492 [34]. The set-up is shown in Fig. 4. The correspondence of this test method with the natural diffusion of chloride ions has been validated previously [52,53]. The mortar specimens were at the ages of 28, 105, 182 and 370

and 730 days. Vacuum-saturation was performed on the mortar specimens with saturated $Ca(OH)_2$ solution. During RCM tests the chloride ions were forced to migrate into the specimens by an external electrical potential (30 V). Three specimens of each mixture were tested simultaneously. After a limited test duration, e.g. 24 h, the specimens were axially split. A 0.1 M $AgNO_3$ solution was sprayed on the freshly split surface. When the white AgCl, precipitated on the surface, was clearly visible, the chloride penetration depth was measured from the center to both edges at intervals of 10 mm.

The non-steady-state migration coefficient of the saturated mortar specimens, noted as D_{Sat} [$\times 10^{-12}$ m^2/s], is calculated with the following equation:

$$D_{\mathrm{Sat}} = \frac{0.0239(237+T)L}{(U-2)t}\left(x_{\mathrm{d}} - 0.0238\sqrt{\frac{(237+T)Lx_{\mathrm{d}}}{U-2}}\right) \tag{5}$$

where U [V] is the absolute value of the applied voltage; T [˚C] is the average value of the initial and final temperatures in the anolyte solution; L [mm] is the thickness of the specimen; x_{d} [mm] is the average value of the penetration depths; t [h] is the test duration.

The measured D_{Sat} -value is commonly used to indicate the capacity of saturated cementitious materials to resist chloride penetration.

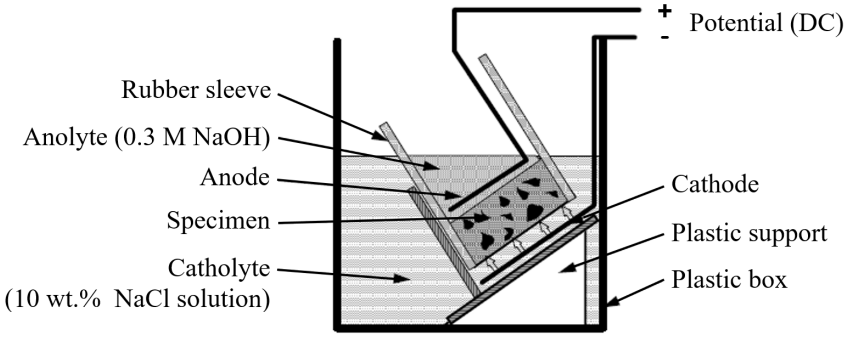

Fig. 4 Set-up for rapid chloride migration test (after NT Build 492 [34]).

4. Results and discussion

4.1 Evolution of pore structure

The pore size distributions of the six paste mixtures as shown in Table 1 were determined by MIP measurements and using the Washburn equation. The results of the FA-blended mixture MF5, as a representative, are presented in Figs. 5 (a) and (b). The total porosity is as

expected decreased with age. A slight decrease of the porosity is found from 182 to 370 days, as shown in Fig. 5a. With a higher age from 28 to 370 days, the pores shift towards a finer distribution. The amount of the large capillary pores (0.08～0.5 μm) is considerably reduced while the amount of the gel pores (< 0.01 μm) is increased, as indicated in Fig. 5b. Between 182 and 370 days, the patterns of the pore size distribution are quite similar (Fig. 5b).

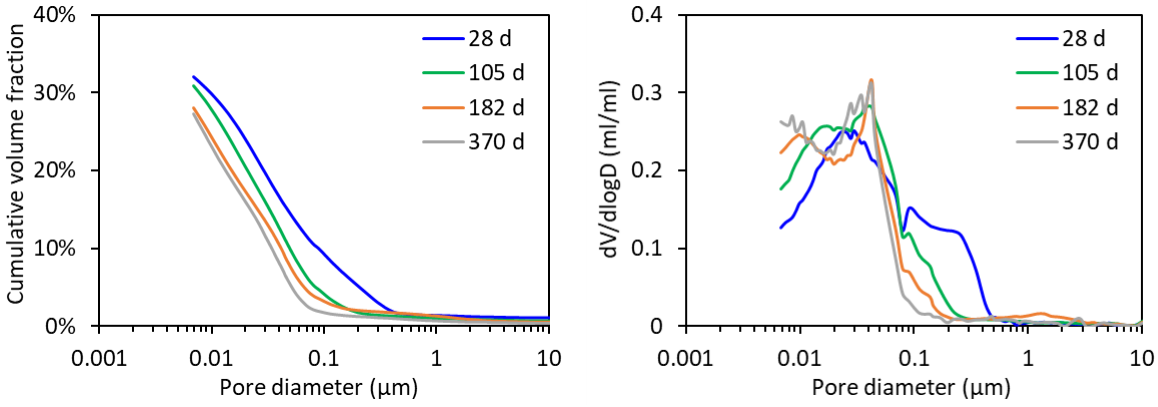

(a) (b)

Fig. 5 Evolution of (a) cumulative pore volume and (b) differential curve with age for FA-blended pastes MF5 (w/b = 0.5).

The average pore diameter d_a, representing the pore size fineness and often-adopted to simplify an arbitrary porous system as a transport tube [3], was determined according to the pore size distribution results and using Eq. (4). Fig. 6 shows the evolution of the d_a value in cementitious paste specimens with age. Each value was determined based on at least three replicates and the standard deviation was within 5.1% for all binders. At 28 days the ternary binder MFL5 has the largest d_a value while the binary binder MB5 has the smallest d_a value. Compared with the reference OPC binder M5, the FA-blended binder MF5 has a lower d_a at 28 days, but shows a similar d_a after 105 days. The binder MFL5 exhibits a larger d_a at 28 days but a slightly smaller d_a after 105 days as compared to the binder M6. It appears that the differences of the d_a between various binders are diminished with age from 28 to 370 days. As can be deduced from Fig. 6, changes of the d_a are very small after one year. This holds for all the binders under study. From regression analysis on experimental data, the evolution of the average pore diameter $d_a(t)$ can be described with an exponential decay function as shown in Eq. (6).

$$d_a(t) = d_0 + A \cdot \exp\left(-\frac{t}{t_0}\right) \qquad (t \geq 28 \text{ days}) \qquad (6)$$

where d_0, A and t_0 are fitting parameters.

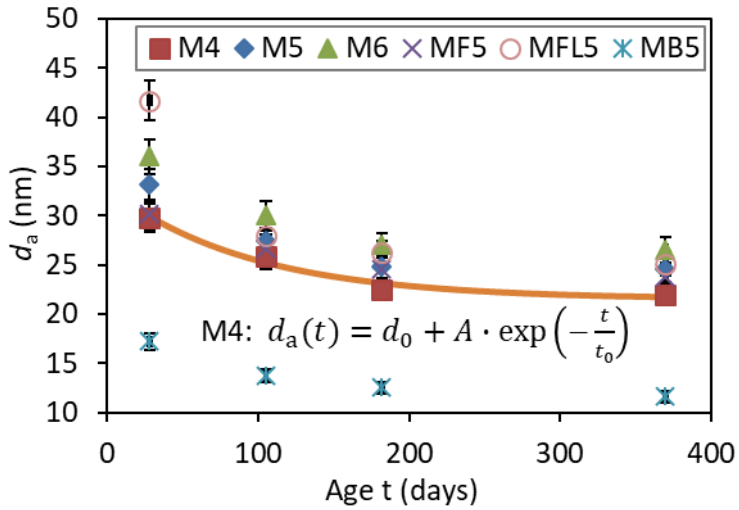

Fig. 6 Evolution of the average pore diameter d_a with age obtained from MIP tests. Mixtures: M4 (OPC, w/b = 0.4), M5 (OPC, w/b = 0.5), M6 (OPC, w/b = 0.6), MF5 (FA 30%, w/b = 0.5), MB5 (BFS 70%, w/b = 0.5), MFL5 (FA 30% + LP 5%, w/b = 0.5).

4.2 Evolution of chloride diffusion coefficient

The chloride diffusion coefficients of cementitious mortars at saturated state, D_{Sat}, were derived from RCM tests. Fig. 7 shows the changes of the D_{Sat} with age from 28 days up to 2 years in saturated mortar specimens. Each D_{Sat} value was the average of three parallel measurements, with a maximum standard deviation of 6.9% for all binders. The roles of w/b ratio and SCMs are under study. In general, the D_{Sat}-value is decreasing in the first 105 days. Particularly for the mortars containing 30% FA (MF5, MFL5), the D_{Sat} drops drastically during this period and their values at 105 days are almost five times smaller than those at 28 days. The mortar containing 70% BFS (MB5) exhibits a high chloride resistance, with the D_{Sat}-value at 28 days approximately four times smaller than that of OPC mortar (M5).

For OPC mortars the D_{Sat}-values show a slight increasing trend after 182 days, while decreasing slowly again from one year onward. The reason for the increase of the D_{Sat}-value remains a pending issue. One possible explanation is the delayed ettringite formation (DEF) [38]. It is worthwhile to note that all the mortar specimens were cured in a humid climate (RH > 98%). Under such circumstances leaching of the alkali hydroxide from the mortar

specimens into the surrounding water can take place and, subsequently, reduces the alkali hydroxide concentration of the mortar pore solutions. The DEF process can be triggered as a consequence of such alkali leaching effect [54,55].

For all blended mortars the D_{Sat}-values decrease slowly after 182 days. After one year the mortars blended with 30% FA (MF5) or with 70% BFS (MB5) have an almost equal resistance to chloride penetration. By comparing the D_{Sat}-values in LP-filled ternary mortar (MFL5) and LP-free binary mortar (MF5), it is found that the presence of 5% LP slightly decreases the D_{Sat}-value in the period from 28 days to 2 years.

Based on regression analysis, and considering the basic evolution of microstructure [38,44], an exponential decay function as shown in Eq. (7) can be used to describe the experimental data of the time-dependent diffusion coefficient $D_{\mathrm{Sat}}(t)$.

$$D_{\mathrm{Sat}}(t) = D_0 + A \cdot \exp\left(-\frac{t}{t_0}\right) \qquad (t \geq 28 \text{ days}) \qquad (7)$$

where D_0, A and t_0 are fitting parameters.

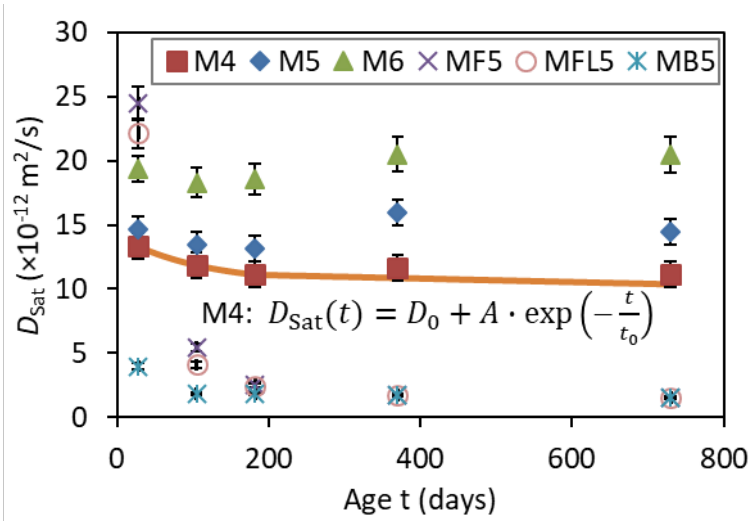

Fig. 7 Evolution of the chloride diffusion coefficient D_{Sat} with age obtained from RCM tests. M4 (OPC, w/b = 0.4), M5 (OPC, w/b = 0.5), M6 (OPC, w/b = 0.6), MF5 (FA 30%, w/b = 0.5), MB5 (BFS 70%, w/b = 0.5), MFL5 (FA 30% + LP 5%, w/b = 0.5).

4.3 Evolution of unsaturated chloride diffusion coefficient

The evolution of the chloride diffusion coefficient $D(t, S_{\mathrm{w}})$ with age (28 days → 50 years) at various degrees of water saturation S_{w} was predicted by Eq. (3), with $d_{\mathrm{a}}(t)$ and $D_{\mathrm{Sat}}(t)$

according to Eqs. (6) and (7), respectively. Note that for a particular age the $D(t, S_w)$ values at various saturation levels S_w were obtained based on the same pore structure, i.e. same average pore diameter d_a was adopted. The obtained $D(t, S_w)$ values for different mortar mixtures are given in Fig. 8.

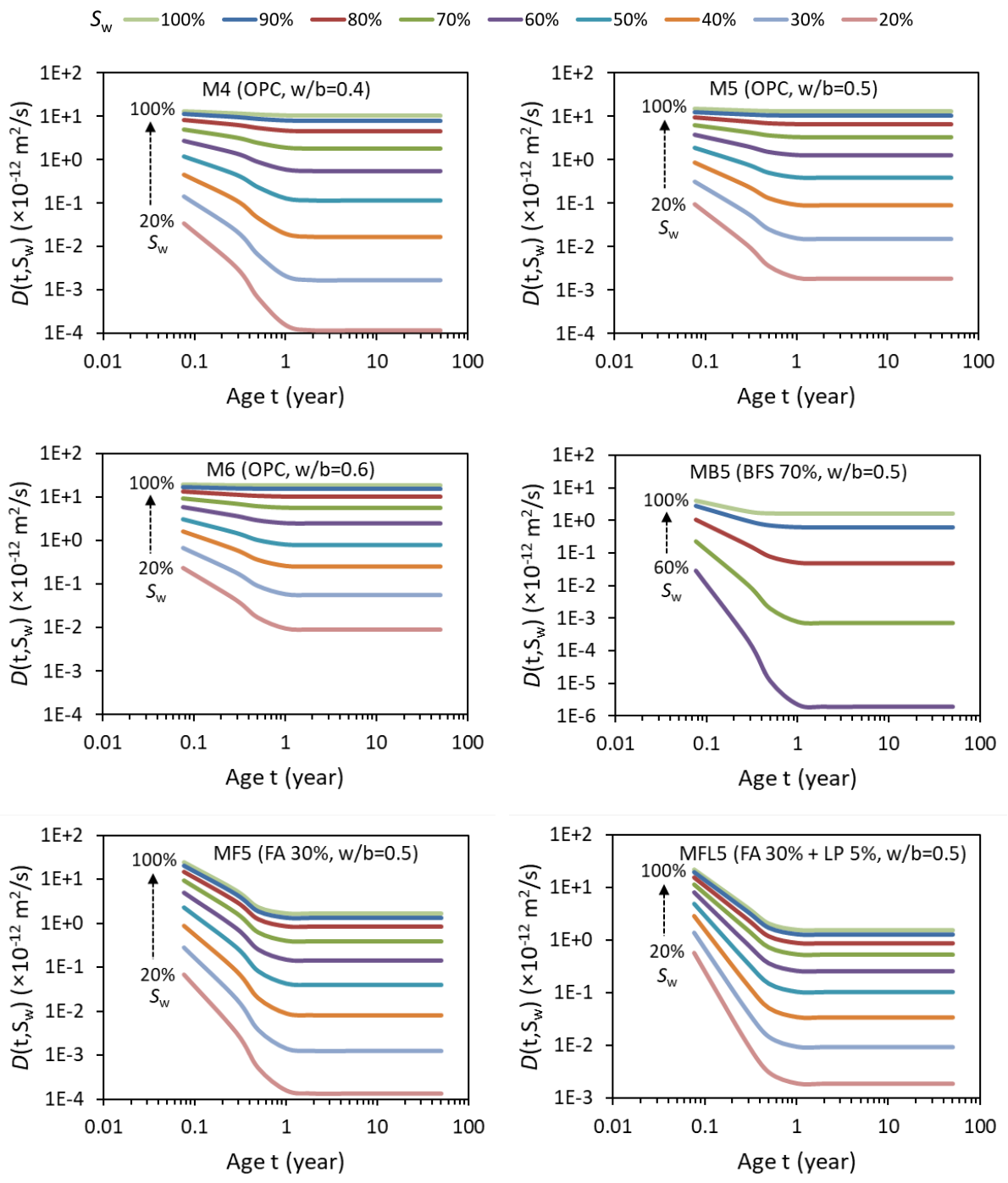

Fig. 8 Evolution of the chloride diffusion coefficient $D(t, S_w)$ with age (28 days → 50 years) in the cementitious mortars at various degrees of water saturation S_w.

For all binders, similar characteristics can be observed in Fig. 8. The chloride diffusion coefficient D generally decreases with age, especially in the first year. At saturated state (S_w = 100%) the diffusion coefficient D exhibits a relatively small decrease with age. The decrease of the diffusion coefficient D, however, becomes increasingly pronounced with decreasing saturation level S_w. It is well known that as hydration proceeds there is a concomitant reduction in water content because the pore water is progressively combined as components of solid hydrates. Hence at longer ages the saturation level S_w will play an increasingly important role in the diffusion coefficient D.

4.3.1 Effect of w/b ratio on $D(t, S_w)$

Fig. 9 presents the chloride diffusion coefficient $D(t, S_w)$ in the OPC mortars with w/b ratios of 0.4, 0.5 and 0.6. The data are taken from Fig. 8. At saturated state (S_w = 100%) the diffusion coefficient D decreases slightly with age after 28 days, whereas at unsaturated state (S_w = 60%) the diffusion coefficient D drops rapidly until the end of the first year. It is revealed that the time-dependency of the D-value is influenced substantially by the saturation level S_w. Such time-dependency is stronger for a lower S_w.

A higher w/b ratio results in a higher diffusion coefficient D, regardless of the degree of water saturation S_w. The effect of the w/b ratio on the D value, however, is much more significant in unsaturated mortars (S_w = 60%) than in saturated mortars (S_w = 100%). By increasing the w/b ratio from 0.4 (M4) to 0.6 (M6), the diffusion coefficient D is approximately 1.7 times higher for S_w = 100%, compared to 4.3 times for S_w = 60%.

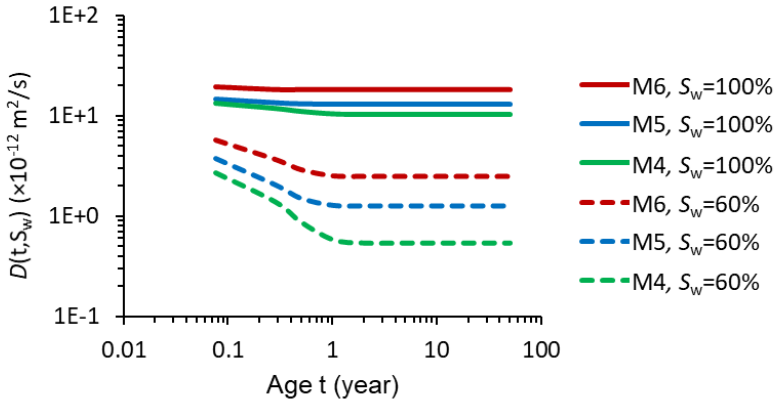

Fig. 9 Chloride diffusion coefficient $D(t, S_w)$ in the saturated (S_w = 100%) and unsaturated (S_w = 60%) OPC mortars with w/b ratios of 0.4 (M4), 0.5 (M5) and 0.6 (M6).

4.3.2 Effect of SCMs on $D(t, S_w)$

Fig. 10 shows the effect of SCMs on the chloride diffusion coefficient $D(t, S_w)$ for saturated (S_w = 100%) and unsaturated (S_w = 70%) mortar specimens. The data come from Fig. 8. Regardless of the binders, a longer term and sharper decrease of the diffusion coefficient D with age is found for S_w = 70% than for S_w = 100%, a similar finding as already drawn from Fig. 9.

For a given water content, either saturated or unsaturated, the blended mortars (MF5, MB5 and MFL5) exhibit lower diffusion coefficient D than the OPC mortar (M5) after 1 year. At saturated state (S_w = 100%) the addition of 30% FA (MF5) or 70% BFS (MB5) results in almost the same diffusion coefficient D at an age of 1 year. At unsaturated state (S_w = 70%), however, the diffusion coefficients D between MF5 and MB5 differ significantly. Compared to binary mortar MF5, the ternary mortar MFL5 shows slightly lower diffusion coefficient D at S_w = 100% (regardless of the age) but obviously higher diffusion coefficient D at S_w = 70% (after 1 year). These observations make it reasonable to consider that in the process of durability design the selection of cementitious materials based on D-values at saturated state can be very different from that based on D-values at non-saturated state. Since onsite cementitious materials are often unsaturated, it is highly advised to examine the unsaturated chloride diffusion coefficient when comparing the durability of structures made with different cementitious materials.

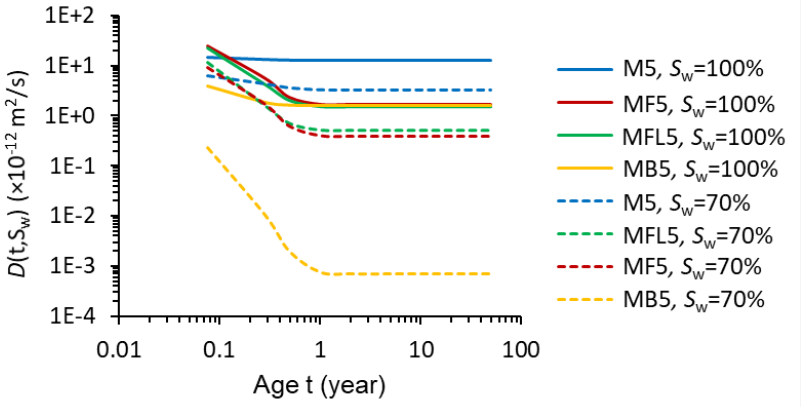

Fig. 10 Chloride diffusion coefficient $D(t, S_w)$ in saturated (S_w = 100%) and unsaturated (S_w = 70%) blended mortars. M5 (OPC, w/b = 0.5), MF5 (FA 30%, w/b = 0.5), MB5 (BFS 70%, w/b = 0.5), MFL5 (FA 30% + LP 5%, w/b = 0.5).

Both Figs. 9 and 10 reveal that for a particular pore structure change, due to either hydration or varying w/b ratio or addition of SCMs, changes of the diffusion coefficient $D(t, S_w)$ are more pronounced at unsaturated state (S_w < 100%) than at saturated state (S_w = 100%). This is acceptable in view of the main path for ionic diffusion in pore systems. When a slight change of pore structure (due to e.g. hydration) occurs in the saturated pore system (Fig. 11a), the main path for ionic diffusion changes slightly, resulting in a slight change of the diffusion coefficient D. However, when a slight change of pore structure occurs in the partially saturated pore system (Fig. 11b), the rate of ionic diffusion can be impaired significantly because of the decreased thickness (from t_1 to t_2) of the layers of capillary water adsorbed on the partially water-filled pores (or channels). Note that the large pore, as depicted in Fig. 11, can be a large channel in 3D microstructure.

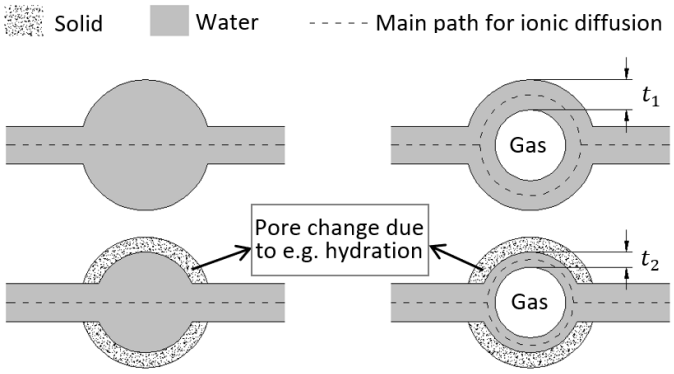

(a) Saturated (b) Partially saturated

Fig. 11 Schematic illustrations on the effect of a minor pore structure change on ionic diffusion in (a) saturated and (b) partially saturated pore systems.

The observation that the dependence of chloride diffusion on pore structure is more pronounced in non-saturated pore system than in saturated pore system can be supported as well by a recent experimental study [56]. There, it has been found that for cementitious systems hydrated beyond 28 days the w/b ratio and SCMs influence the pore connectivity mainly by altering the connectivity of small capillary pores while the connectivity of large capillary pores is not influenced much. Under saturated state, the large capillary pores can have a great contribution to ionic transport. With decrease of saturation level S_w, the role of the small capillary pores in ionic transport becomes increasingly prominent and, subsequently, the pore structures made with different w/b ratios or SCMs can exhibit even larger differences in the diffusion coefficient D.

Therefore, it is reasonable to conclude that the non-saturated state tends to promote a longer term and sharper decrease of the diffusion coefficient D than the saturated state.

5. Comparative study

A comparison on evolutions of the unsaturated chloride diffusion coefficient with age is made between the present approach (Eq. (3)) and the DuraCrete approach [33]. The comparative study highlights the significance of the degree of water saturation in the service life prediction of concrete structures in chloride-laden environments. In the following the impact of moisture transport on ionic diffusion phenomenon is not considered in the calculations of *long-term* chloride penetration [31,41,42].

5.1 Specimens and exposure condition

For the sake of simplification, the study concerns two cementitious mortars exposed to atmospheric marine condition. Table 2 shows the mixtures and properties of the two mortars. The relative humidity RH of the atmospheric marine condition changes in the range of 65~90% within each year, with an average annual RH of 77.5% [11].

Table 2 Details of two mortar mixtures; $D_{\mathrm{Sat,28days}}$ is the chloride diffusion coefficient obtained from RCM tests of 28-day-old saturated mortar specimens.

Mortars	Binders	w/b	$D_{\mathrm{Sat,28days}}$ ($\times 10^{-12}$ m^2/s)
M5	OPC	0.5	14.71
MB5	OPC 30% + BFS 70%		3.97

5.2 $D(t)$ by DuraCrete approach

In DuraCrete [33] the service life of marine concrete structures relies on Eq. (8), which describes the changes of chloride diffusion coefficient $D(t)$ with age t.

$$D(t) = D_0 \cdot k_{\mathrm{c}} \cdot k_{\mathrm{e}} \cdot \left(\frac{t_0}{t}\right)^n \tag{8}$$

where D_0 [m^2/s] is the chloride diffusion coefficient at a reference age t_0; k_{c} is the curing factor (k_{c} = 0.79 when t_0 = 28 days); n is the ageing factor; k_{e} is the environment factor, which depends on environment class $k_{\mathrm{e},0}$ and type of cement $k_{\mathrm{e,c}}$:

$$k_{\mathrm{e}} = k_{\mathrm{e},0} \cdot k_{\mathrm{e,c}} \tag{9}$$

452 The values of the ageing factor n and the sub-factors ($k_{\mathrm{e},0}$ and $k_{\mathrm{e,c}}$) are presented in Table
453 3. DuraCrete follows a probabilistic method as well as partial factors to calculate the
454 probabilities of failure. The details are out of the scope and will not be presented.
455
456 Table 3 Characteristic values of the ageing factor n and the environment factor ($k_{\mathrm{e},0}$ and $k_{\mathrm{e,c}}$)
457 [33].

	Condition	Characteristic values
Ageing factor n	OPC, Submerged	0.30
	OPC, Tidal and splash	0.37
	OPC, Atmospheric	0.65
	BFS, Submerged	0.71
	BFS, Tidal and splash	0.60
	BFS, Atmospheric	0.85
$k_{\mathrm{e},0}$ for environment class	Submerged	1.32
	Tidal zone	0.92
	Splash zone	0.27
	Atmospheric	0.68
$k_{\mathrm{e,c}}$ for type of cement	OPC	1.0
	BFS	2.9

458

459 5.3 $D(t, S_{\mathrm{w}})$ by present approach

460 In the present approach the evolution of the unsaturated chloride diffusion coefficient
461 $D(t, S_{\mathrm{w}})$ with age is determined by Eq. (3), with the values of $d_{\mathrm{a}}(t)$ and $D_{\mathrm{Sat}}(t)$ according to
462 Eqs. (6) and (7), respectively. The degree of water saturation S_{w} is supposed to change with
463 time t when the mortars are exposed to atmospheric marine condition. Assuming a service
464 life of 50 years, Eqs. 10 (a) (b) (c) are introduced to describe the time-related saturation level
465 $S_{\mathrm{w}}(\mathrm{t})$:
466 1) In the first 28 days the mortar specimens are saturated (S_{w} = 100%) (Eq. (10a)).

2) In the service period (28 days → 50 years), the saturation level S_w of the mortar specimens decreases with time (Eq. (10b)). Eq. (10b) is given following the power expression of Eq. (1).

3) At the age of 50 years, each mortar specimen reaches its equilibrium saturation level, $S_{w,e}$, which corresponds to the equilibrium humidity level approximately the same as the average annual RH of the atmospheric air, i.e. 77.5% RH. At this RH level the $S_{w,e}$ can be estimated from the water vapor desorption isotherm (WVDI) of each mortar. The WVDI results can be referred to a previous study reported in Ref. [57], where the $S_{w,e}$ values are 55% and 83% for mortars M5 and MB5, respectively.

$$S_w(t) = 100\% \qquad 0 \le t \le 0.0767 \text{ year (28 days)} \qquad (10a)$$

$$S_w(t) = S_{w,t=0.0767} \cdot \left(\frac{0.0767}{t}\right)^m \qquad 0.0767 < t < 50 \text{ years} \qquad (10b)$$

$$S_w(t) = S_{w,e} \qquad t = 50 \text{ years} \qquad (10c)$$

where m is a constant. By combining Eq. (10c) with Eq. (10b), the m-values are determined as 0.092 and 0.029 for mortars M5 and MB5, respectively. Fig. 12 shows the time-related saturation level $S_w(t)$ obtained with Eqs. 10 (a) (b) (c) for OPC and BFS-blended mortars.

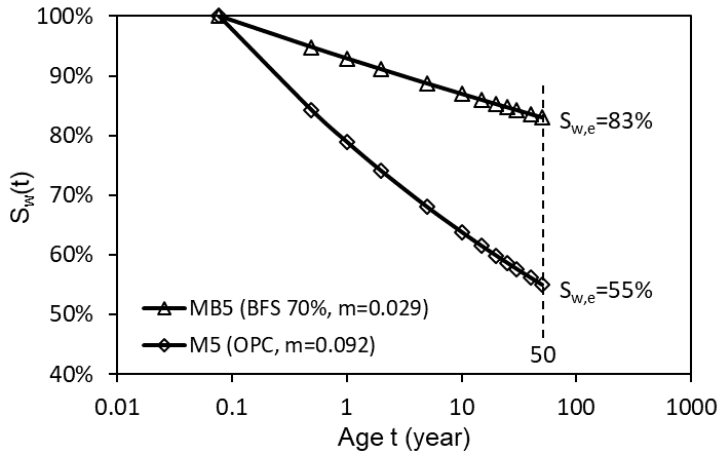

Fig. 12 Time-related degree of water saturation $S_w(t)$ for atmospheric OPC and BFS-blended mortars following Eqs. 10 (a) (b) (c).

Figs. 13 (a) and (b) present the chloride diffusion coefficient $D(t, S_w)$ at different saturation levels S_w for OPC mortar M5 and BFS-blended mortar MB5, respectively. The data come from Fig. 8. In the cases when the saturation level S_w decreases with time by following Eqs. 10 (a) (b) (c), the evolution of $D(t, S_w)$ is replotted in Figs. 13 (a) and (b) with

the dotted black lines. It is shown that the $D(t, S_w)$ value, with the S_w decreasing with age (corresponding to lower S_w with depth as indicated in Fig. 2), drops much more significantly with age compared to that obtained based on saturated mortars (S_w = 100%).

For a comparative study the time-dependent chloride diffusion coefficient $D(t)$ recommended in DuraCrete (Eq. (8)) is also presented in Figs. 13 (a) and (b) with the solid black lines. At any particular age the $D(t)$ value from Eq. (8) is in the same order of magnitude as that determined from Eq. (3). This holds for both OPC and BFS-blended binders. The significant influence of the degree of water saturation on chloride diffusion, hidden behind but not explicitly addressed in DuraCrete, can therefore be clearly demonstrated by Eq. (3) proposed in the present work.

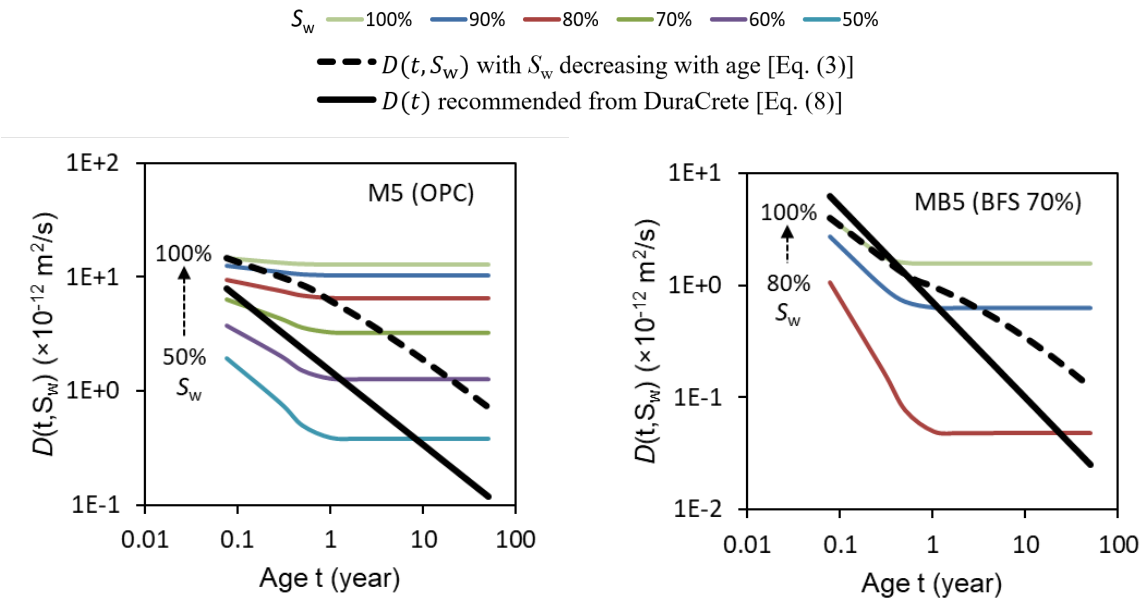

Fig. 13 Evolution of unsaturated chloride diffusion coefficient $D(t, S_w)$ in neat OPC mortar (M5) and BFS-blended mortar (MB5).

Debates have been reported with respect to the ageing factor n. One of the most popular mentioned is that the ageing factor n, as recommended in the DuraCrete, can result in the chloride diffusion coefficient D to become extremely small at long ages and, accordingly, tend to produce a much longer predicted service life than those actually achievable [58]. Based on the comparative study as indicated in Fig. 13, the very small D-value at long ages may be achieved in the sense that the internal part of the onsite concrete is partially saturated. A number of field studies have proved very small diffusion coefficient, $D = 0.9\times10^{-12}$ m^2/s for cement concrete after 24-year service in Gothenburg harbor [59]. Much larger values of the

ageing factor n have been reported based on field studies, e.g. ageing factor up to 0.7 based on chloride profiles for coastal bridges in service up to 37 years [60], than those reported based on RCM tests of laboratory saturated concretes, e.g. ageing factors up to 0.24 [38].

6. Applications and limitations of the proposed approach

The formula of time-dependent unsaturated chloride diffusion coefficient developed in this work, viz. Eq. (3), provides a tool for durability assessment of reinforced concrete structures, even for those of old structures with unknown mixtures. After a reference age t_{ref}, the degree of hydration $\alpha(t)$ changes limited (Fig. 3). The values of $D_{\mathrm{Sat}}(t)$ and $d_{\mathrm{a}}(t)$, as indicated in Eq. (3), will change limited accordingly. The long-term chloride diffusion coefficient will, therefore, primarily rely on the time-dependent degree of water saturation $S_{\mathrm{w}}(t)$.

Field investigations have revealed that the influential depth of water permeation, caused by water storage or wetting-drying cycles, is limited to the outermost few centimeters of the cover concrete and the internal concrete still relies on self-desiccation. Chloride ingression in the surface concrete is fast while that in the internal concrete (which has a low water content) is quite slow. The chloride penetration period required to initiate reinforcement corrosion highly depends on the slow chloride diffusion in the internal unsaturated concrete. Such slow chloride diffusion can be evaluated by Eq. (3), where the values of S_{w} and d_{a}, both changing with age due to self-desiccation, can be estimated from laboratory measurements.

There is a need for long-term inspections and field measurements to capture the moisture profile and its evolution with age in cover concrete under marine environment, in order to accurately predict the chloride transport in the surface part of the concrete, i.e. Zone I as illustrated in Fig. 2. Moreover, existing works such as those presented here need to be continued accounting for the impact of water permeation on chloride diffusion. Accumulation of the chloride ions in surface concrete, owing to e.g. wetting-drying cycles, can take place and its effect on unsaturated chloride diffusion is well worth studying.

7. Conclusions

A formula for predicting the evolution of chloride diffusion coefficient in unsaturated cementitious materials is proposed. The significant influence of the degree of water saturation S_{w} on long-term chloride diffusion, hidden behind but not explicitly addressed in DuraCrete, has been substantiated. One of the lessons to be gained from this study is that the S_{w} should

be taken into account when engineers make a final specification for concrete mixes. The effect of the S_w on chloride diffusion is of greater importance than perhaps is commonly considered. The non-saturated state enables to promote a longer term and sharper decrease of chloride diffusion, compared with saturated state. The ageing factor n is significantly influenced by the S_w.

The effects of factors, such as w/b ratio and SCMs, on chloride diffusion coefficient become increasingly pronounced with decreasing S_w. At saturated state the mortars including 70% slag or 30% fly ash, cured after 1 year, have almost equal resistance to chloride diffusion. At non-saturated state, however, the mortar with 70% slag shows obviously smaller chloride diffusion than the mortar with 30% fly ash. Compared to the binary mortar (70% OPC + 30% fly ash), the ternary mortar (65% OPC + 30% fly ash + 5 % limestone powder) shows slightly smaller chloride diffusion at saturated state but obviously larger chloride diffusion at non-saturated state (e.g. S_w = 70%).

The results call into question the use of the chloride diffusion coefficient of saturated concretes, obtained from current standard diffusion/migration tests, when onsite concretes are actually partially saturated. A continuation of this work will consider the effect of water permeation on chloride transport. Within the scope of this work, an accurate service life prediction is not expected. The present work has the intension to emphasize the significance of the degree of water saturation in determinations of the ageing factor n and long-term transport properties in marine concrete.

Acknowledgements

This work was supported by the Minjiang Scholar Program of Fujian province, China (grant No. Min-jiaogao[2018]-56, GXRC-19045), the Natural Science Foundation of Fujian province (grant No. 2019J01235), the Fuzhou Science and Technology Bureau (grant No. 2018-G-78) and the Talent-Introduction Program of Fuzhou University (grant No. GXRC-19023). Sincere appreciation goes to Prof. Klaas van Breugel (Delft University of Technology) for his insightful comments and valuable suggestions.

References

[1] Zhang Y, Zhang M. Transport properties in unsaturated cement-based materials – a review. Constr Build Mater 2014; 72:367-379.

574 [2] Zhang Y, Zhang M, Ye G. Influence of moisture condition on chloride diffusion in
575 partially saturated ordinary Portland cement mortar. Mater Struct 2018; 51:36.
576 [3] Zhang Y, Ye G. A model for predicting the relative chloride diffusion coefficient in
577 unsaturated cementitious materials. Cem Concr Res 2019; 115:133-144.
578 [4] Zhang Y, Ye G, Yang ZX. Dependence of unsaturated chloride diffusion on the pore
579 structure in cementitious materials. Unpublished results.
580 [5] Tang LP, Nilsson L-O. Chloride binding capacity and binding isotherms of OPC
581 pastes and mortars. Cem Concr Res 1993; 23:242-253.
582 [6] Justnes H, De Weerdt K, Geiker MR. Chloride binding in concrete exposed to
583 seawater and salt solutions, in: Li ZJ, Sun W, Miao CW, Sakai K, Gjørv OE, Banthia
584 N (Eds.), Proc 7th Int Conf Concrete under Severe Loading (CONSEC), RILEM
585 Proceedings PRO 84Nanjing, China; 2013; 1:647-659.
586 [7] Tang LP. Concentration dependence of diffusion and migration of chloride ions Part 1.
587 Theoretical considerations. Cem Concr Res 1999; 29:1463-1468.
588 [8] Tang LP. Concentration dependence of diffusion and migration of chloride ions Part 2.
589 Experimental evaluations. Cem Concr Res 1999; 29:1469-1474.
590 [9] Andrade C. Concepts on the chloride diffusion coefficient. Third RILEM workshop
591 on Testing and Modelling the Chloride Ingress into Concrete, 9-10 September 2002,
592 Madrid, Spain.
593 [10] Collepardi M, Marcialis A, Turriziani R. The kinetics of penetration of chloride ions
594 into the concrete (in Italian), Il Cemento 1970:157-164.
595 [11] Saetta AV, Scotta RV, Vitaliani RV. Analysis of chloride diffusion into partially
596 saturated concrete. ACI Mater J 1993; 90(5):441-451.
597 [12] Johannesson BF. A theoretical model describing diffusion of a mixture of different
598 types of ions in pore solution of concrete coupled to moisture transport. Cem Concr
599 Res 2003; 33:481-488.
600 [13] Swaddiwudhipong S, Wong SF, Wee TH, Lee SL. Chloride ingress in partially and
601 fully saturated concretes. Concr Sci Eng 2000; 2:17-31.
602 [14] Tang LP, Nilsson L-O, Basheer PAM. Resistance of concrete to chloride ingress:
603 Testing and modelling. Spon Press; 2012.
604 [15] Poulsen E, Mejlbro L. Diffusion of chloride in concrete: Theory and application,
605 Taylor & Francis, London & New York; 2006.

606 [16] Climent MA, de Vera G, Lopez JF, Viqueira E, Andrade C. A test method for
607 measuring chloride diffusion coefficients through non-saturated concrete: Part I. The
608 instantaneous plane source diffusion case. Cem Concr Res 2002; 37:714-724.
609 [17] Nielsen EP, Geiker MR. Chloride diffusion in partially saturated cementitious
610 material. Cem Concr Res 2003; 33:133-138.
611 [18] Nilsson L-O. Present limitations of models for predicting chloride ingress into
612 reinforced concrete structures. J Phys IV France 2006; 136:123-130.
613 [19] Olsson N, Lothenbach B, Baroghel-Bouny V, Nilsson L-O. Unsaturated ion diffusion
614 in cementitious materials – The effect of slag and silica fume. Cem Concr Res 2018;
615 108:31-37.
616 [20] Olsson N, Baroghel-Bouny V, Nilsson L-O, Thiery M. Non-saturated ion diffusion in
617 concrete – A new approach to evaluate conductivity measurements. Cem Concr
618 Compos 2013; 40:40-47.
619 [21] Zhou CS, Chen W, Wang W, Skoczylas F. Indirect assessment of hydraulic
620 diffusivity and permeability for unsaturated cement-based material from sorptivity.
621 Cem Concr Res 2016; 82:117-129.
622 [22] Ahs M, Nilsson L-O, Haha MB. A method to determine the critical moisture level for
623 unsaturated transport of ions. Mater Struct 2015; 48:53-65.
624 [23] Samson E, Marchand J. Modeling the transport of ions in unsaturated cement-based
625 materials. Comput Struct 2007; 85:1740-1756.
626 [24] Voinitchi D, Julien S, Lorente S. The relation between electrokinetics and chloride
627 transport through cement-based materials. Cem Concr Compos 2008; 30:157-166.
628 [25] Zhang P, Wittmann FH, Vogel M, Müller HS, Zhao T. Influence of freeze-thaw
629 cycles on capillary absorption and chloride penetration into concrete. Cem Concr Res
630 2017; 100:60-67.
631 [26] Zhang P, Wittmann FH, Lura P, Müller HS, Han S, Zhao T. Application of neutron
632 imaging to investigate fundamental aspects of durability of cement-based materials: A
633 review. Cem Concr Res 2018; 108:152-166.
634 [27] Chatterji S, Kawamura M. Electrical double layer, ion transport and reactions in
635 hardened cement paste. Cem Concr Res 1992; 5:774-782.
636 [28] Chatterji S. Transportation of ions through cement based materials-Part 1:
637 Fundamental equations and basic measurement techniques. Cem Concr Res 1994; 24
638 (5):907-912.

639 [29] Yang YK, Wang MR. Pore-scale modeling of chloride ion diffusion in cement
640 microstructures. Cem Concr Compos 2018; 85:92-104.
641 [30] Takewaka K, Mastumoto S. Quality and cover thickness of concrete based on the
642 estimation of chloride penetration in marine environments, in: V.M. Malhotra (Ed.),
643 Proc. 2nd Int Conf Concr Marine Envir, ACI SP-109, 1988:381-400.
644 [31] Mangat PS, Molloy BT. Prediction of long term chloride concentration in concrete.
645 Mater Struct 1994; 27:338-346.
646 [32] Tang L, Nilsson L-O. Chloride diffusivity in high strength concrete at different ages.
647 Nordic Concr Res 1992; 11:162-171.
648 [33] DuraCrete R17, DuraCrete Final Technical Report, The European Union – Brite
649 EuRam III, DuraCrete – Probabilistic Performance based Durability Design of
650 Concrete Structures, Document BE95-1347/R17, May 2000; CUR, Gouda, the
651 Netherlands.
652 [34] NT Build 492 – Nordtest Method, Chloride migration coefficient from non-steady
653 state migration experiments. 1999.
654 [35] Scrivener KL, Nonat A. Hydration of cementitious materials, present and future. Cem
655 Concr Res 2011; 41(7):651-665.
656 [36] Tang L. Electrically accelerated methods for determining chloride diffusivity in
657 concrete. Mag Concr Res 1996; 48(176):173-179.
658 [37] Baert G, Gruyaert E, Audenaert K, De Belie N. Chloride ingress in high-volume fly
659 ash concrete. 1st Int Conf on Microstructure Related Durability of Cementitious
660 Composites, 13-15 October 2008, Nanjing, China. ed. Sun W, van Breugel K, Miao C,
661 Ye G and Chen H, Print-ISBN: 978-2-35158-065-3, e-ISBN: 978-2-35158-084-4,
662 Publisher: RILEM Publications; 2008:473-482.
663 [38] Yu ZQ. Microstructure development and transport properties of Portland cement-fly
664 ash binary systems-in view of service life predictions. PhD Thesis, Delft University of
665 Technology, the Netherlands; 2015.
666 [39] Persson B. Self-desiccation and its importance in concrete technology. Mater Struct
667 1997; 30(5):293–305.
668 [40] Nilsson L-O. Interaction between microclimate and concrete - a prerequisite for
669 deterioration. Constr Build Mater 1996; 10:301-308.
670 [41] Fraj BA, Bonnet S, Khelidj A. New approach for coupled chloride/moisture transport
671 in non-saturated concrete with and without slag. Constr Build Mater 2012; 35:761-
672 771.

673 [42] Li K, Li C, Chen Z. Influential depth of moisture transport in concrete subject to
674 drying–wetting cycles. Cem Concr Compos 2009; 31(10):693-698.
675 [43] Baroghel-Bouny V, Nguyen TQ, Dangla P. Assessment and prediction of RC
676 structure service life by means of durability indicators and physical/chemical models.
677 Cem Concr Compos 2009; 31(8):522–534.
678 [44] Zhang Y. Non-saturated chloride diffusion in sustainable cementitious materials. PhD
679 thesis, Delft University of Technology, the Netherlands; 2018.
680 [45] Zhang Y, Ouyang XW, Yang ZX. Microstructure-based relative humidity in
681 cementitious system due to self-desiccation. Mater 2019;12(8):1214.
682 [46] Chatterji S. On the applicability of Fick's second law to chloride ion migration
683 through Portland cement concrete. Cem Concr Res 1995; 25:299–303.
684 [47] Nilsson L-O et al. HETEK, A system for estimation of chloride ingress into concrete,
685 Theoretical background. The Danish Road Directorate, Copenhagen, 1996, Report No.
686 83.
687 [48] Chrisp TM, McCarter WJ, Starrs G, Basheer PAM, Blewett J. Depth-related variation
688 in conductivity to study cover-zone concrete during wetting and drying. Cem Concr
689 Compos 2002; 24:415–426.
690 [49] Jonasson J-E. Slipform construction - calculations for assessing protection against
691 early freezing. Swedish Cement and Concrete Research Institute, Stockholm; 1984;
692 4:84.
693 [50] Washburn EW. Note on method of determining the distribution of pore size in porous
694 materials. Proc Natl Acad Sci 1921; 7:115–116.
695 [51] Zhang Y, Yang B, Yang Z, Ye G. Ink-bottle effect and pore size distribution of
696 cementitious materials identified by pressurization–depressurization cycling mercury
697 intrusion porosimetry. Mater 2019; 12:1454.
698 [52] Tang L, Nilsson L-O. Rapid determination of chloride diffusivity of concrete by
699 applying an electric field. ACI Mater J 1992, 89:49–53.
700 [53] Andrade C. Calculation of chloride diffusion coefficients in concrete from ionic
701 migration measurements. Cem Concr Res 1993; 23:724-742.
702 [54] Famy C. Expansion of heat-cured mortars. PhD thesis, Imperial College of Science,
703 Technology, and Medicine; 1999.
704 [55] Diamond S. The relevance of laboratory studies on delayed ettringite formation to
705 DEF in field concretes. Cem Concr Res 2000; 30(12):1987-1991.

706 [56] Zhang Y, Ye G. Characterization of pore structure in cementitious materials by
707 intrusion-extrusion cyclic mercury porosimetry (IEC-MIP). Symposium on Concrete
708 Modelling and Material Behaviour (CONMOD2018), Delft, the Netherlands; 2018.
709 [57] Zhang Y, Ye G. Chloride transport in partially saturated mortar made of blended
710 cement, Conference: 14th Int Congress on the Chemistry of Cement (ICCC2015),
711 13~16 October, Beijing, China; 2015.
712 [58] Bentz DP, Feng XP. Time-dependent diffusivities: possible misinterpretation due to
713 spatial dependence. Testing and Modelling the Chloride Ingress into Concrete. Proc
714 2nd Int RILEM Workshop. September 11-12, Paris, France; 2000:225-233.
715 [59] Fidjestøl P, Justnes H. Long-term experience with microsilica concrete in a marine
716 environment. Nord Concr Res 2004; 31(1):30-39.
717 [60] Maage M, Helland S, Poulsen E, Vennesland Ø, Carlsen JE. Service life prediction of
718 existing concrete structures exposed to marine environment. ACI J 1996; 93(6):602-
719 608.